QUANTUM AND OPTICAL ARITHMETIC AND FRACTALS

M.V. BERRY
H. H. Wills Physics Laboratory,
Tyndall Avenue, Bristol BS8 1TL, UK

Three waves depend on a common mathematical structure. The waves are light beyond a diffraction grating with sharp-edged slits, initially transversely uniform microwaves propagating along a strip guide, and the evolving probability amplitude for a quantum particle in a one-dimensional box where the initial state is a constant. The mathematical structure is the indefinite integral over ξ of

$$K(\xi,\tau)=\sum_{n=-\infty}^{\infty}\exp\left\{\mathrm{i}\pi\left[2\xi\left(n+\frac{1}{2}\right)-\tau\left(n+\frac{1}{2}\right)^2\right]\right\}$$

which is a theta function (Gauss sum) on its natural boundary. For rational τ, the integral is piecewise constant and describes fractional quantum revivals and the fractional Talbot effect. For irrational τ, the graph of the wave intensity as a function of ξ is a fractal with dimension 3/2. As a function of τ, the graph has dimension 7/4. On some diagonal lines (space-time sections in quantum mechanics), e.g. $\xi=(1-\tau)/2$, the dimension is 5/4.

1 Introduction

Claude Itzykson excelled in finding physical applications for sophisticated concepts and techniques from number theory. I think he would have enjoyed the physics described here, in which arithmetic and fractal geometry appear in a way that was surprising at first and then gave new insights into the simplest quantum time-dependence and the distribution of light in a waveguide and beyond a diffraction grating. I will give only a brief description; details and generalizations can be found in two recent papers[1,2].

My aim is to describe geometrical structures in the sum

$$\Psi(\xi,\tau)=\frac{2}{\pi}\sum_{n=0}^{\infty}\frac{(-1)^n}{(n+\frac{1}{2})}\cos\left\{2\pi\xi\left(n+\frac{1}{2}\right)\right\}\exp\left\{-\mathrm{i}\pi\tau\left(n+\frac{1}{2}\right)^2\right\} \quad (1)$$

In a first interpretation, this satisfies the time-dependent Schrödinger equation

$$\mathrm{i}\partial_\tau\Psi(\xi,\tau)=-\frac{1}{4\pi}\partial_\xi^2\Psi(\xi,\tau) \quad (2)$$

with the boundary condition

$$\Psi\left(\pm\frac{1}{2},\tau\right)=0 \tag{3}$$

and the initial condition

$$\Psi(\xi,0)=\frac{2}{\pi}\sum_{n=0}^{\infty}\frac{(-1)^n}{\left(n+\frac{1}{2}\right)}\cos\left\{2\pi\xi\left(n+\frac{1}{2}\right)\right\}=1\quad\left(|\xi|<\frac{1}{2}\right) \tag{4}$$

It follows that Ψ describes what is perhaps the simplest nonstationary quantum bound state, where an initially spatially constant wavefunction evolves inside a unit box (infinite potential well). Taken together, (3) and (4) imply that the initial state is discontinuous at the walls $\xi=\pm 1/2$, a fact that will have interesting consequences.

A different interpretation of (2) is as the paraxial wave equation in two-dimensions, with τ as a longitudinal spatial variable and ξ the transverse variable. This gives solutions to the Helmholtz equation with wavenumber k and wavelength $\lambda=2\pi/k$, namely

$$\left(\partial_x^2+\partial_z^2+k^2\right)\phi(x,z)=0 \tag{5}$$

with the variables related by

$$\begin{gathered}x=a\xi,\quad z=z_{\mathrm{T}}\tau,\quad \phi(x,z)\approx\exp(\mathrm{i}kz)\,\Psi(\xi,\tau)\\ \text{where } z_{\mathrm{T}}\equiv\tfrac{a^2}{\lambda} \text{ and } a \text{ is a length}\end{gathered} \tag{6}$$

Here, the approximation is paraxial, that is it describes waves travelling close to the z axis, in a sense that will be made more precise later. With this reinterpretation, (1) describes the wave propagating inside a waveguide in the form of a unit strip with Dirichlet boundary conditions at the edges $x=\pm a/2$, where the wave is spatially uniform as it enters the guide.

A further interpretation is provided by the wave

$$\Psi_1(\xi,\tau)\equiv\frac{1}{2}\left[1+\Psi(2\xi,4\tau)\right] \tag{7}$$

which also satisfies (2) and with (5) and (6) can be interpreted as a paraxial wave in the half-plane $(0\leq x\leq\infty)$, $(-\infty<z<\infty)$. This is periodic in ξ with period 1, and satisfies the condition

$$\Psi_1(\xi,0) = 1 \left(\text{if } |\xi \bmod 1| < \frac{1}{4}\right) \qquad (8)$$
$$= 0 \left(\text{if } |\xi \bmod 1| > \frac{1}{4}\right)$$

It follows that Ψ_1 describes the paraxial propagation of a plane wave of light, initially travelling in the ζ direction, after passage at $\zeta = 0$ through a diffraction grating with period $\Delta\xi = 1$, that is $\Delta x = a$, consisting of opaque and transparent strips with equal widths; this is called a Ronchi grating.

In what follows, repeated use will be made of the following obvious symmetries of the wave (1):

$$\Psi(\xi,-\tau) = \Psi^*(\xi,\tau);\ \Psi(\xi,\tau+1) = \exp\{-i\pi/4\}\,\Psi(\xi,\tau);$$
$$\text{i.e. } \Psi(\xi,1-\tau) = \exp\{-i\pi/4\}\,\Psi^*(\xi,\tau);$$
$$\Psi(-\xi,\tau) = \Psi(\xi,\tau);\ \Psi(\xi+1,\tau) = -\Psi(\xi,\tau); \qquad (9)$$
$$\text{i.e. } \Psi(1-\xi,\tau) = -\Psi(\xi,\tau)$$

2 Revivals and Talbot images

It follows from (9) that at integer times τ the probability density

$$P(\xi,\tau) \equiv |\Psi(\xi,\tau)|^2 \qquad (10)$$

repeatedly reconstructs its initially constant form. This is the simplest example[3] of the much more general phenomenon of *quantum revivals*[4,5], in which a wide class of initial quantum states (for example, representing electrons in atoms) get approximately reconstructed at integer multiples of a time that depends on the spectrum and the form of the initial state.

For the diffraction grating wave (7), the analogous statement is

$$\Psi_1(\xi,\tau+1) = \frac{1}{2}\left[1 - \Psi(2\xi,4\tau)\right] = \Psi_1\left(\xi+\frac{1}{2},\tau\right) \qquad (11)$$

Therefore at integer multiples p of the distance z_T in (6), the grating profile (8) is reconstructed by the diffracted light, with a half-period shift if p is odd. This repeated self-imaging is the *Talbot effect*[6-8], and z_T is the Talbot distance. The Talbot effect is also a more general phenomenon that is embodied in (7),

because (paraxially) perfect imaging occurs not only for the Ronchi grating (8) but for any profile.

Now consider the quantum wave Ψ at rational times $\tau = p/q$, where p and q are mutually prime integers. It is helpful to write this as the integral over the propagator K for the particle in a box. Thus

$$\Psi(\xi,\tau) = \int_{-1/2}^{1/2} d\xi_0 K(\xi-\xi_0,\tau),$$

$$\text{where } K(\xi,\tau) = \sum_{n=-\infty}^{\infty} \exp\left\{i\pi\left[2\xi\left(n+\frac{1}{2}\right)-\tau\left(n+\frac{1}{2}\right)^2\right]\right\} \quad (12)$$

Now set $\tau = p/q$, and split the sum into groups of q terms by defining[9]

$$n = lq + s \quad (-\infty < l < \infty, 1 \le s \le q) \quad (13)$$

The crucial observation is that the exponential involving l^2 can be simplified, because

$$\exp\{-i\pi pql^2\} = \exp\{-i\pi q e_p l\}$$

$$\text{where } e_p = 1\,(p \text{ even}) \text{ or } 0\,(p \text{ odd}) \quad (14)$$

This enables the sum over l to be evaluated as a series of δ functions, to give, after some reduction,

$$K\left(\xi,\frac{p}{q}\right) = \frac{1}{\sqrt{q}} \sum_{n=-\infty}^{\infty} A_n(q,p)\,\delta\left(\xi - \frac{1}{2}\left(e_p+\frac{p}{q}\right)-\frac{n}{q}\right) \text{ where} \quad (15)$$

$$A_n(q,p) = \frac{1}{\sqrt{q}} \exp\left\{i\pi\left(\frac{p}{4q}+\frac{e_p}{2}+\frac{n}{q}\right)\right\} \sum_{s=1}^{q} \exp\left\{i\frac{\pi}{q}\left((2n+qe_p)s-ps^2\right)\right\}$$

When combined with the integral (12), this result shows that the wave for these rational times is the (piecewise constant) superposition of q shifted overlapping copies (labelled by n) of the initial wave in the box (set equal to zero outside). These are *fractional quantum revivals*[3,4]. The nature of the superposition is determined by the A_n, which are easily shown to be pure phase factors, that is

$$A_n(q,p) = \exp\{i\Phi_n(q,p)\} \tag{16}$$

The phases Φ_n can be evaluated by recognizing the formula for A_n in (15) as a variant of the Gauss sum of number theory; explicit formulae can be found elsewhere[1,2,9].

Figure 1 shows fractional revivals of the probability density for increasing q, as $\tau = p/q$ takes values given by successive approximations to the golden mean. These were computed as the sum of q shifted copies with the phases Φ_n. Confirmation of the correctness of the analysis was obtained by computing Ψ for the same τ with the eigenfunction series (1), which gave exactly the same pictures (apart from Gibbs oscillations smoothing the discontinuities, caused by truncating the series).

The optical analogues of the fractional revivals are the *fractional Talbot images*[10,11] at distances $z = z_T\ p/q$ from the grating. In each unit cell (e.g. $0 \le x \le a$), these images are superpositions, with phases Φ_n, of q copies of the grating, with amplitudes reduced by $1/\sqrt{q}$. The above-mentioned explicit formulae for the phases considerably facilitate the calculation of these images.

3 Fractal waves

Rational values of τ are special. For typical (i.e. irrational) τ, and, more generally, as a function of the variables ξ and τ, the Schrödinger wave Ψ defined by (1) - and also the diffraction grating wave Ψ_1 defined by (7) - possesses rich fractal properties. These are conveniently described by the fractal dimensions of the graphs of the probability density (10) along lines in spacetime, that is, in the ξ, τ plane.

In calculating the various fractal dimensions[12], I will apply to $\Psi(\xi,\tau)$ a result for Fourier series

$$f(u) = \sum_m a_m \exp\{imu\} \tag{17}$$

where the a_m have random or pseudorandom phases. If the power spectrum $|a_m|^2$ has the asymptotic form

$$|a_m|^2 \sim |m|^{-\beta}\ as\ |m| \to \infty, \text{where } 1 < \beta \le 3, \tag{18}$$

then the graphs of Ref and Imf are continuous but nondifferentiable, with fractal dimension

$$D_f = \frac{1}{2}(5-\beta) \tag{19}$$

Thus $\beta = 3$ corresponds to a (just) differentiable curve with $D_f = 1$, and $\beta = 1$ would correspond to an area-filling curve with $D_f = 2$. Equation (17) can be obtained (by simple dimensional analysis) from the result[13] that if f has dimension D_f the mean square increment of $f(u)$ over a infinitesimal distance Δu is proportional to $(\Delta u)^{4-2D_f}$; for a straightforward derivation of this result, see[14]. This applies when D_f represents the capacity dimension, but in the present context I expect it to hold for the Hausdorff and other fractal dimensions as well[15]. Elsewhere[2] I have argued that the fractal dimension of the graph of $|f(u)|^2$ is, almost always, also D_f. Therefore the fractal properties of $\mathrm{Re}\,\Psi$ and $\mathrm{Im}\,\Psi$ are inherited by the probability density $P(\xi, \tau)$.

At irrational times τ, when quantum revivals do not occur, the quantum wave Ψ, regarded as a function of position ξ in the box, has the form (17), with Fourier components $m = (n+1/2)$ and pseudorandom phases $\pi\tau m^2$. The power spectrum is, from (1), proportional to m^{-2}, so that $\beta = 2$ in (18) and, from (19), the fractal dimension of the probability density is $D_\xi = 3/2$. The same argument gives the dimension of the graph of wave intensity across the strip waveguide, and of the light intensity beyond a Ronchi grating in almost all planes, where z/z_T is irrational and there are no fractional Talbot images.

Figure 1 shows how the spatial quantum fractal for $\tau = \tau_G = (3 - \sqrt{5})/2$ emerges as the limit of sequences of fractional revivals corresponding to the continued-fraction (Fibonacci) approximants to τ_G. Figure 2 shows the spatial fractal for $\tau = 1/2\pi$ in greater detail, and a magnification illustrating the self-similarity. Pictures for other irrational τ, and for the Talbot image intensity $|\Psi_1|^2$, are similar.

Now consider Ψ as a function of time τ, at fixed position ξ. As has been explained, the probability density derived from the wave (1) is periodic in τ. Its Fourier series contains longitudinal frequencies restricted to the values $m = (n+1/2)^2$. For such a lacunary series, the power spectrum is $|a_n|^2 \mathrm{d}n/\mathrm{d}m$, which is proportional to $m^{-3/2}$. In the argument following (17) we now have $\beta = 3/2$, giving the unexpected fractal dimension $D_\tau = (5 - \beta)/2 = 7/4$. This is not restricted to rational ξ, and indeed we think the probability density is a fractal function of time everywhere, except at the walls $\xi = \pm 1/2$. Figure 3 shows one of these time fractals, and a magnification illustrating its self-similarity. The greater fractal dimension, reflected in the greater irregularity of these curves in comparison with those in figure 2, is clear.

The time and space fractals can be seen together in figure 3, which is a landscape plot of $P(\xi, \tau)$. Evidently this is not an amorphous fractal, but contains much additional structure. In particular, unanticipated diagonal lines can be discerned, corresponding to particular spacetime slices through the P landscape (one is visible issuing from the rear right of the picture; with

other views of the landscape[2], more are visible). As I have described in detail elsewhere[2], these form part of an infinite set of lines, namely

$$\xi = m\tau + n + \frac{1}{2}\ (m \neq 0)\,, \quad \xi = \left(m + \frac{1}{2}\right)\tau + \frac{1}{2}n \quad (m, n \text{ integer}) \qquad (20)$$

on which partial destructive interference between the terms in (1) reduces the fractal dimension to $D_{\text{diag}} = 5/4$. One of these spacetime fractals is shown in figure 5; it is noticeably less irregular than either of the previous fractals, reflecting its smaller dimension. The lines (20) also appear as 'canals' in the analogous computations for Gaussian wavepackets[3].

Further analysis of the sum (1) may reveal more fractal treasures, for example spacetime lines (not necessarily straight) on which more complicated interference between groups of terms leads to fractal probability densities with dimensions different from D_τ, D_ξ, or D_{diag}.

4 Discussion.

In the wave behind a diffraction grating, several of the phenomena so far discussed, namely the Talbot images for rational z/z_T, the transverse fractals with dimension 3/2, for irrational z/z_T, and the 'longitudinal' fractals with dimension 7/4, as z varies for fixed x, have been observed in a recent experiment[1]. At first it seems surprising that it is possible to see the transverse fractal dimension 3/2, because any misorientation of the plane of observation, such as must surely occur in reality, ought to give a light intensity pattern whose fractal dimension is that of a generic section, namely the larger value 7/4. That the transverse fractal can in fact be seen is the result of a curious combination of two circumstances, and could hold a more general message for the interpretation of experiments involving fractals.

The first is that the Talbot fractals possess infinitely fine detail only in the limit of perfect paraxiality, unlike the quantum fractals that are exact solutions of Schrödinger's equation. A detailed analysis[1] shows that this is the limit $\lambda/a \to 0$. Finite values of λ/a give rise to postparaxial blurring of the transverse and longitudinal detail in the fractals (and the edges of the rational Talbot images) according to the same function that gives diffraction smoothing of the cusp caustic of geometrical optics. (This echo of geometrical asymptotics is curious - albeit mathematically unsurprising - in view of the fact that the sharp detail that is being postparaxially blurred is itself the result of (paraxial) wave interference).

The second circumstance is that the natural 'unit cell' of the Talbot effect, namely $\Delta_x = a$, $\Delta z = z_T$, is enormously elongated relative to the dimensionless unit cell $\Delta\xi = 1$, $\Delta\tau = 1$ (by a factor a/λ, which in the experiment reported in [1] was 803). This effect causes any misorientation of the observation plane in x, z space to be greatly reduced in ξ, τ space, often to such a degree that it falls within the postparaxial τ blurring. So, paradoxically, the transverse fractal is rendered observable because fine detail in the longitudinal fractal is obscured. The same argument suggests -again paradoxically- that the elongation of the natural cell should make it more difficult to see the dimensionally dominant longitudinal fractal; nevertheless, observation was possible, by careful alignment exploiting the symmetry of the Talbot images about $\xi = 0$.

The Talbot fractals are not restricted to Ronchi gratings, but will occur, with the same dimensions $D_\xi = 3/2$ and $D\tau = 7/4$, whenever the transmission function has discontinuities in its amplitude and phase.

For the quantum fractals, the situation described here can be generalized enormously[2], to quantum waves evolving in arbitrary D-dimensional enclosures with $D-1$ dimensional boundaries, from arbitrary initial states with discontinuities. It would seem that the chaology of geodesics (trivially integrable in a one-dimensional box) might dominate the fractal geometry of the evolution, since fine detail depends on high-lying eigenstates, that is on semiclassical asymptotics. But in fact the results have a wider universality: whatever the chaology, the graph of the probability density as a function of time at a fixed position is a fractal curve with dimension 7/4, and the graph as a function of position for fixed time is a $D + 1/2$ dimensional fractal hypersurface. These results do not apply if the boundary of the enclosure is itself a fractal, with dimension $D - 1 + \gamma$ (where $0 < \gamma < 1$); then, a physical argument suggests that the time fractal dimension is $(7 + \gamma)/4$, and the space fractal dimension is $D + (1 + \gamma)/2$. Further generalizations can easily be envisaged.

The simple wave $\Psi(\xi, \tau)$ (equation 1) is the indefinite integral (cf. 12) of a Jacobi theta function (infinite Gauss sum)[16], on the natural boundary of its domain of convergence: if τ had a small negative imaginary part, the sum in (12) would converge. Although the theta function does not converge, the singular behaviour on its natural boundary is reflected in the rich structure of fractals and quantum revivals in its integral Ψ, which does converge. The theta functions themselves would arise in the evolution of quantum waves from a δ-function initial condition, or from a grating of infinitely narrow slits. In the optical case there are two principal effects that would make the analogue of the sum converge. First, there is non-paraxiality, mentioned already. Second, there is the effect of the finite number N of slits in any real grating, giving rise to a wave described by a finite Gauss sum. As $N \to \infty$, the wave in irrational

planes z/z_T gets infinitely complicated, in a way that can be fully described by a chaotic renormalization transformation[17].

Finally, it is worth remarking how different are the superficially analogous problems involving the heat equation, obtained by analytic continuation of τ to the negative imaginary axis. Then (1) describes the evolution of temperature in a bar where the initial temperature is constant and the ends are maintained at a different constant temperature. In this situation the sum (1), and the associated theta function, converge exponentially, and there are no revivals and no fractals.

References

1. Berry, M.V. *J. Modern Optics* in press, (1996).
2. Berry, M.V. *J. Phys. A* submitted, (1996).
3. Stifter, P., Leichtle, C., Lamb, W.E. & Schleich, W.P. *in preparation* (1996).
4. Averbukh, I.S. & Perelman, N.F. *Physics Letters A* **139**, 449-453 (1989).
5. Mallalieu, M. & Stroud, C.R.J. *Phys. Rev. A.* **51**, 1827-1835 (1995).
6. Talbot, H., F. *Phil. Mag.* **9**, 401-407 (1836).
7. Rayleigh, L. *Phil. Mag.* **11**, 196-205 (1881).
8. Patorski, K. *Progress in Optics* **27**, 1-108 (1989).
9. Hannay, J.H. & Berry, M.V. *Physica* **1D**, 267-290 (1980).
10. Hiedemann, E.A. & Breazale, M.A. *J. Opt. Soc. Amer.* **49**, 372-375 (1959).
11. Winthrop, J.T. & Worthington, C.R. *J. Opt. Soc. Amer.* **55**, 373-381 (1965).
12. Mandelbrot, B.B. *The Fractal Geometry of Nature* (Freeman, San Francisco, 1982).
13. Orey, S. Z. *Warsch. verw. Geb.* **15**, 249-256 (1970).
14. Berry, M.V. & Lewis, Z.V. *Proc.Roy.Soc.* **A370**, 459-484 (1980).
15. Falconer, K. *The geometry of fractal sets: mathematical foundations and applications* (Wiley, New York, 1990).
16. Gradshteyn, I.S. & Ryzhik, I.M. *Table of Integrals, Series and Products* (Academic Press, New York and London, 1980).
17. Berry, M.V. & Goldberg, J. *Nonlinearity* **1**, 1-26 (1988).

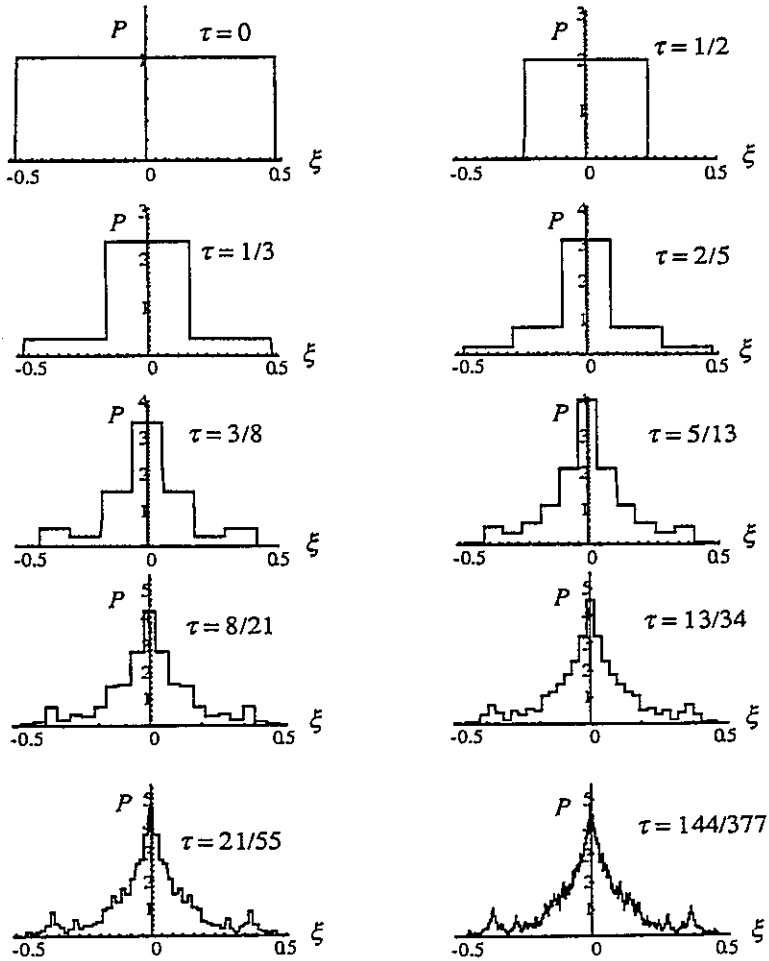

Figure 1. Probability density $P(\xi,\tau)=|\Psi(\xi,\tau)|^2$ for a particle in a box, at the indicated times τ, approximating the golden mean $\tau_G=(3-\sqrt{5})/2 = 0.381966$ ($\approx 144/377+3.15\times10^{-6}$), showing fractional quantum revivals accumulating to give the spatial fractal, with dimension $D_\xi=3/2$.

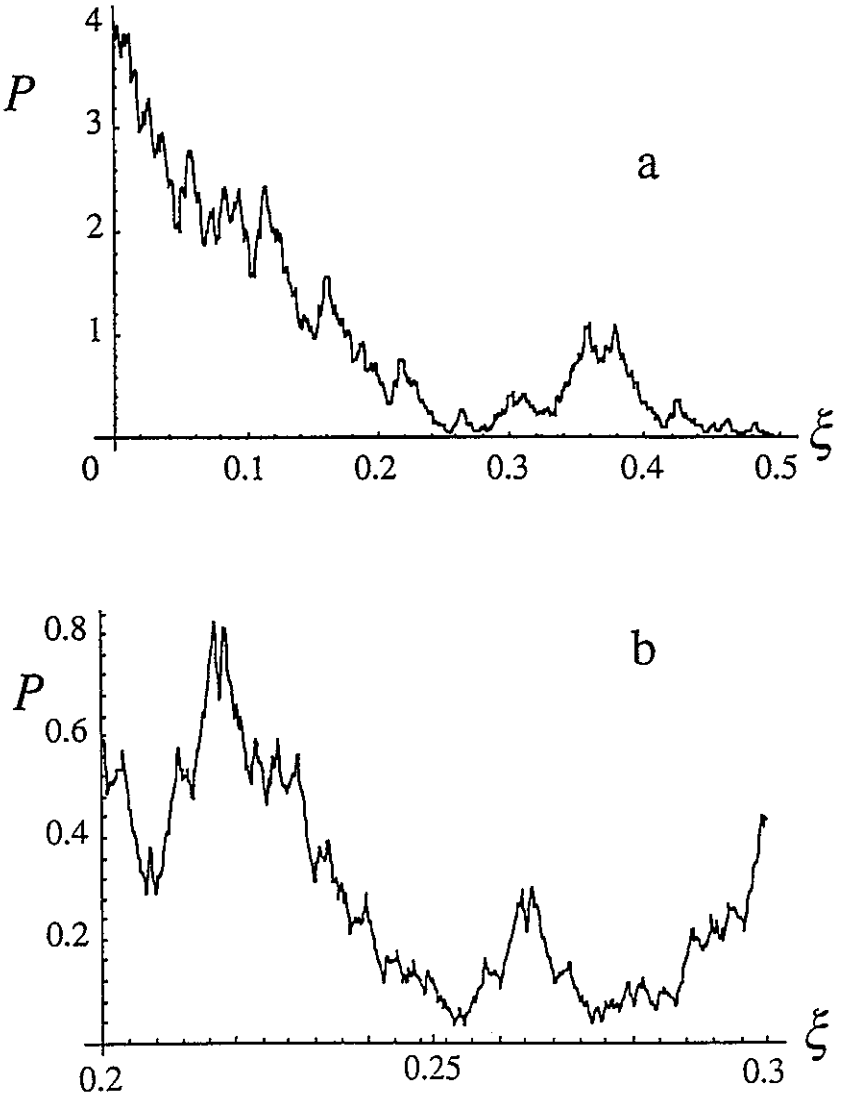

Figure 2. Quantum spatial fractal for $\tau=1/e$. (a): over the irreducible range $0\leq\xi\leq 1/2$, and (b): magnified to show the self-similarity.

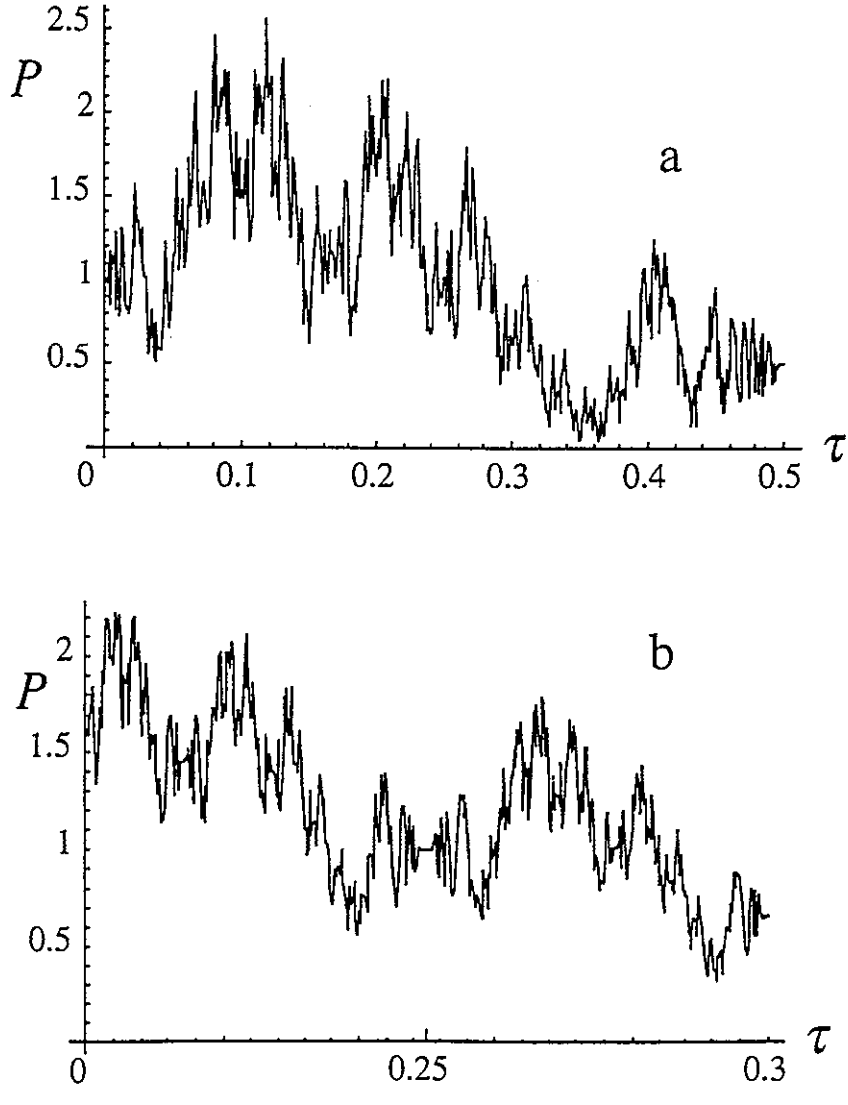

Figure 3. Quantum time fractal, with dimension $D_\tau=7/4$, for $\xi=0.25$; (a): over the irreducible range $0\leq\tau\leq1/2$, and (b): magnified to show the self-similarity.

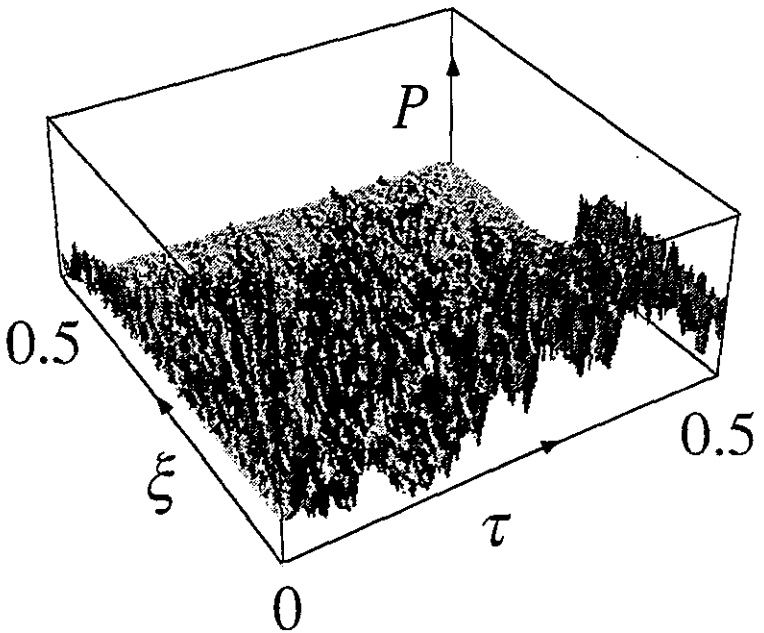

Figure 4. Illuminated landscape plot of the fractal probability density $P(\xi,\tau)$ in time and space for a particle in a box.

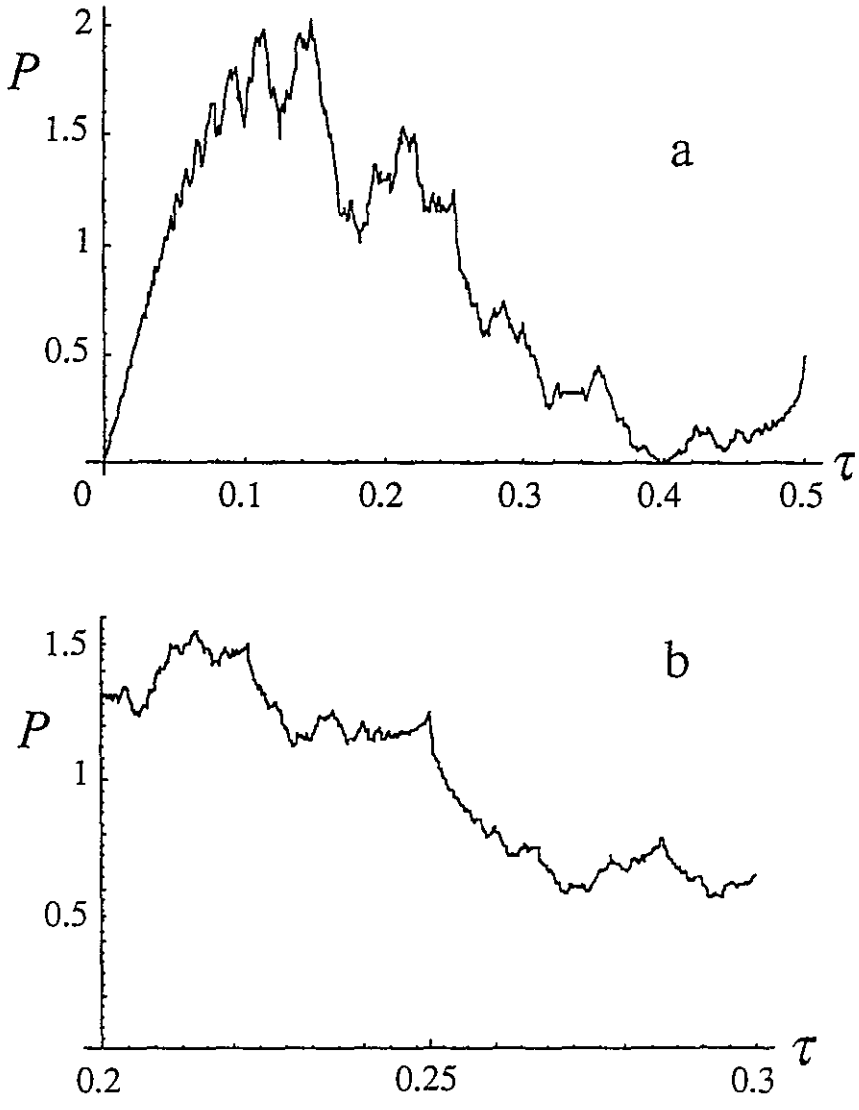

Figure 5. Quantum diagonal fractal, with dimension $D_{diag}=5/4$, for the spacetime slice $\xi=(5\tau+1)/2$; (a): over the range $0\leq\tau\leq 1/2$, and (b): magnified to show the self-similarity.